Terra Nova

doi: 10.1111/ter.12177

Messinian events in the Black Sea

Christiaan G. C. van Baak,[1] Eleanora P. Radionova,[2] Larisa A. Golovina,[2] Isabella Raffi,[3] Klaudia F. Kuiper,[4] Iuliana Vasiliev[1] and Wout Krijgsman[1]

[1]*Paleomagnetic Laboratory "Fort Hoofddijk", Utrecht University, Budapestlaan 17, Utrecht 3584CD, The Netherlands;* [2]*Geological Institute, Russian Academy of Sciences (RAS), Pyzhevsky per. 7, Moscow 119017, Russia;* [3]*Department of Engineering and Geology, Università "G. d'Annunzio", Via dei Vestini 31, Chieti Scalo 66013, Italy;* [4]*Faculty of Earth and Life Sciences, Vrije Universiteit Amsterdam, De Boelelaan 1085, Amsterdam 1081 HV, The Netherlands*

ABSTRACT

Past hydrological interactions between the Mediterranean Sea and Black Sea are poorly resolved due to complications in establishing a high-resolution time frame for the Black Sea. We present a new greigite-based magnetostratigraphic age model for the Mio-Pliocene deposits of DSDP Hole 380/380A, drilled in the southwestern Black Sea. This age model is complemented by $^{40}Ar/^{39}Ar$ dating of a volcanic ash layer, allowing a direct correlation of Black Sea deposits to the Messinian salinity crisis (MSC) interval of the Mediterranean Sea. Proxy records divide these DSDP deposits into four intervals: (i) Pre-MSC marine conditions (6.1–6.0 Ma); (ii) highstand, fresh to brackish water conditions (~6.0–5.6 Ma); (iii) lowstand, fresh-water environment (5.6–5.4 Ma) and (iv) highstand, fresh-water conditions (5.4–post 5.0 Ma). Our results indicate the Black Sea was a major fresh-water source during gypsum precipitation in the Mediterranean Sea. The introduction of Lago Mare fauna during the final stage of the MSC coincides with a sea-level rise in the Black Sea. Across the Mio-Pliocene boundary, sea-level and salinity in the Black Sea did not change significantly.

Terra Nova, 27, 433–441, 2015

Introduction

Connectivity between the Mediterranean and the Paratethys region to the north was important during the Messinian salinity crisis (5.97–5.33 Ma) (e.g. Roveri *et al*., 2014). The Messinian Paratethys comprised large parts of the drainage area of Central Eurasia and formed a water body of similar surface area to the Mediterranean Sea (Popov *et al*., 2006). The Paratethys therefore represents a major source of non-marine water, but its influence on the hydrological budget and the MSC deposits of the Mediterranean is still unknown, mainly because of poor chronological resolution. Recently, Messinian successions in marginal settings in the Dacian and Black Sea basins have been correlated in detail to the MSC deposits (Krijgsman *et al*., 2010; Vasiliev *et al*., 2011, 2013; Stoica *et al*., 2013), but a deep Black Sea record has not yet been resolved.

In 1975, DSDP Leg 42B drilled several holes in the deep Black Sea to study the interactions between the Paratethys and Mediterranean (Fig. 1). One of the most controversial outcomes of this expedition was the discovery of a pebbly mudstone unit (unit IVd in Hole 380/380A), found at a depth of 875 mbsf (Ross, 1978). This unit was interpreted as a shallow water deposit and assumed by some to represent the desiccation of the Black Sea during the MSC (Hsü and Giovanoli, 1979). However, sediments overlying unit IVd were recently shown to be older than the MSC (Grothe *et al*., 2014). This indicates a time-equivalent record of the MSC may be present in the overlying deposits. To complicate matters, recent seismic studies have found evidence of large-scale mass transport complexes in the region (Tari *et al*., 2015).

The lack of independent age constraints in the DSDP Leg 42B cores has long impeded the establishment of a robust time frame for the deep Black Sea deposits. Post-cruise magnetostratigraphic dating was hindered by the little-understood authigenic iron sulphide mineral greigite (Fe_3S_4) being the main magnetic carrier (Giovanoli, 1979). In recent years, the understanding of greigite has significantly improved, and this mineral can, under the right circumstances, be considered a reliable magnetic carrier (Vasiliev *et al*., 2008; Roberts *et al*., 2011; Chang *et al*., 2014). Especially in the circum-Black Sea region, numerous Late Miocene and Pliocene land-based sections with greigite as the magnetic carrier have been magnetostratigraphically dated (Vasiliev *et al*., 2004, 2005, 2011; Krijgsman *et al*., 2010; Van Baak *et al*., 2013). Here, we provide independent age constraints for Hole 380/380A of DSDP Leg 42B and create an improved time frame by magnetostratigraphically and radioisotopically dating the interval overlying unit IVd. This allows us to plot previously published proxy records in time to unravel the coevolution of the Mediterranean and Black Sea during the MSC.

Mediterranean-Paratethys co-evolution

Paratethys-Mediterranean connectivity is determined by the interplay between active tectonics in the palaeo-Bosporus region and changes in Mediterranean sea-level (Cagatay *et al*., 2006). As a result, the Black Sea experienced significant palaeoenvironmental changes in the Late Miocene-Pliocene. During the early

Correspondence: Christiaan van Baak, Paleomagnetic Laboratory "Fort Hoofddijk", Utrecht University, Budapestlaan 17, Utrecht 3584CD, The Netherlands. Tel.: +31 302535246; e-mail: c.g.c.vanbaak@uu.nl

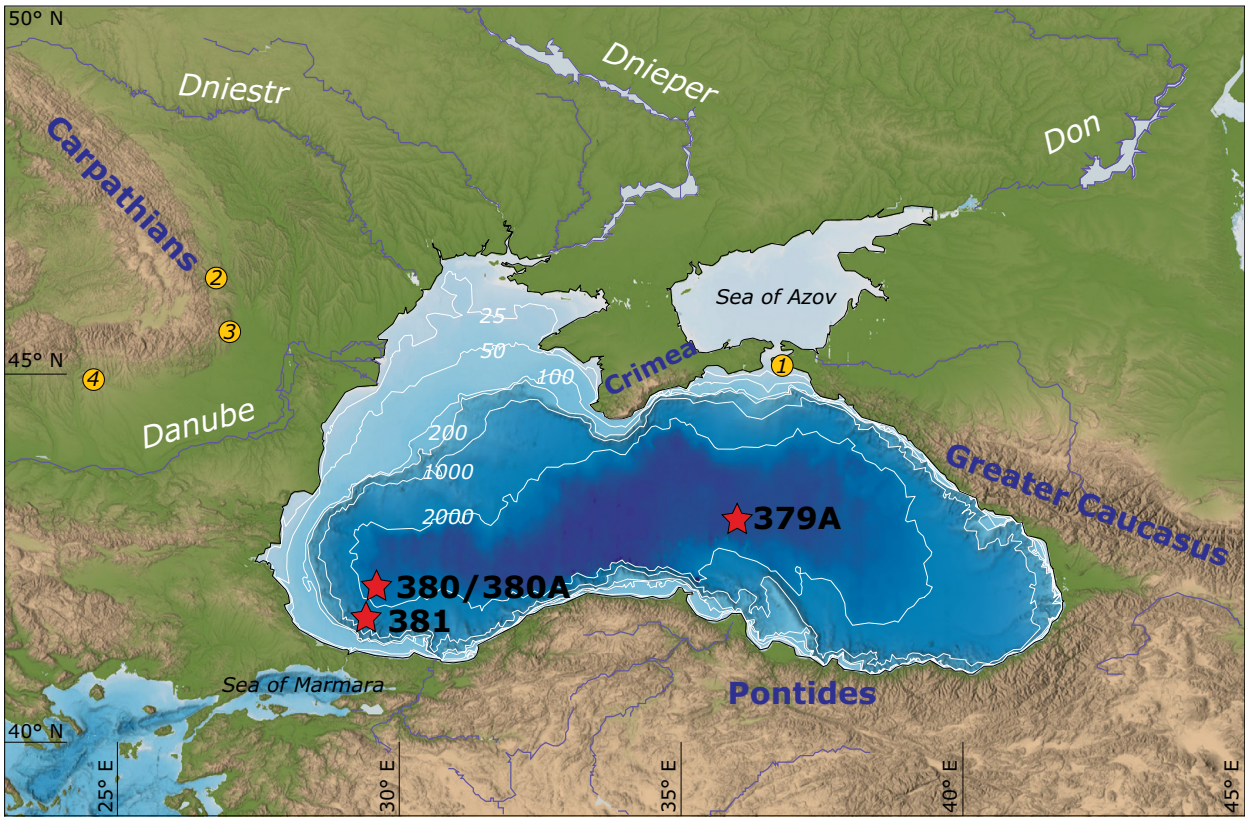

Fig. 1 Map of the locations of the DSDP Leg 42B holes 379A–381 and major geographic features. Numbered circles indicate magnetostratigraphically dated reference sections for the Late Miocene and Plio-Pleistocene. (1) Taman Peninsula, Russia (Krijgsman *et al.*, 2010; Vasiliev *et al.*, 2011); (2) Putna river (Vasiliev *et al.*, 2004); (3) Rimnicu Sarat river (Romania) (Vasiliev *et al.*, 2004); (4) Badislava and Topolog (Vasiliev *et al.*, 2005).

Messinian, the Paratethys experienced both marine and fresh-water conditions (Nevesskaya *et al.*, 2003; Popov *et al.*, 2006; Radionova *et al.*, 2012). At ~6.1 Ma, prior to the onset of the MSC, a connection was established between the Mediterranean and Paratethys (Krijgsman *et al.*, 2010; Chang *et al.*, 2014). A sea-level and salinity rise throughout the Paratethys is evidenced by a brief moment of full marine conditions (Radionova and Golovina, 2011a; Stoica *et al.*, 2013). Highstand conditions with a two-way connection between the Mediterranean and Paratethys continue throughout the first gypsum stage of the MSC (Vasiliev *et al.*, 2013). At the Black Sea margin, the acme of the MSC coincides with a sea-level drop, with the final marine deposit dated at 5.6 Ma (Krijgsman *et al.*, 2010). To better understand the Mediterranean-Paratethys coevolution, a record from the basinal part of the Black Sea is required. DSDP Hole 380/380A is located near the Bosporus on the basin apron at a water depth of 2107 m and may therefore record deposition across the MSC in a deep basinal setting. To understand Black Sea evolution during the MSC, a high-resolution time frame for this site is of vital importance.

Results

Magnetostratigraphy

We follow similar thermal demagnetization techniques on discrete specimens to those previously described by Vasiliev *et al.* (2007). 54 samples were taken between 700 and 875 mbsf. Between 200 and 400 °C, these samples show a consistent component of normal or reverse polarity, comparable to previously analysed greigite-bearing Paratethys rocks (Fig. 2). Between 700 and 780 mbsf, three zones of both reverse and normal (N1, N2, N3) polarity are found. Below 780 mbsf a long reverse-polarity zone continues down to 845 mbsf, where one sample has a clear normal direction. Below 845 mbsf, in units IVc and IVd, this temperature component becomes weaker and difficult to interpret, resulting in undetermined polarities.

$^{40}Ar/^{39}Ar$ dating

At 706.8 mbsf, a 2 cm thick dacitic tuff layer is present (Shipboard Scientific Staff, 1978). A feldspar fraction with a grainsize between 90 and 250 μm and a density between 2.54 and 2.59 g cm^{-3} was isolated using standard mineral separation techniques. The sample was irradiated for 18 h at the Petten High Flux Reactor (The Netherlands) in the Cd-shielded RODEO-P3 position. $^{40}Ar/^{39}Ar$ measurements were performed on a Helix-MC noble gas mass spectrometer. We calculated an

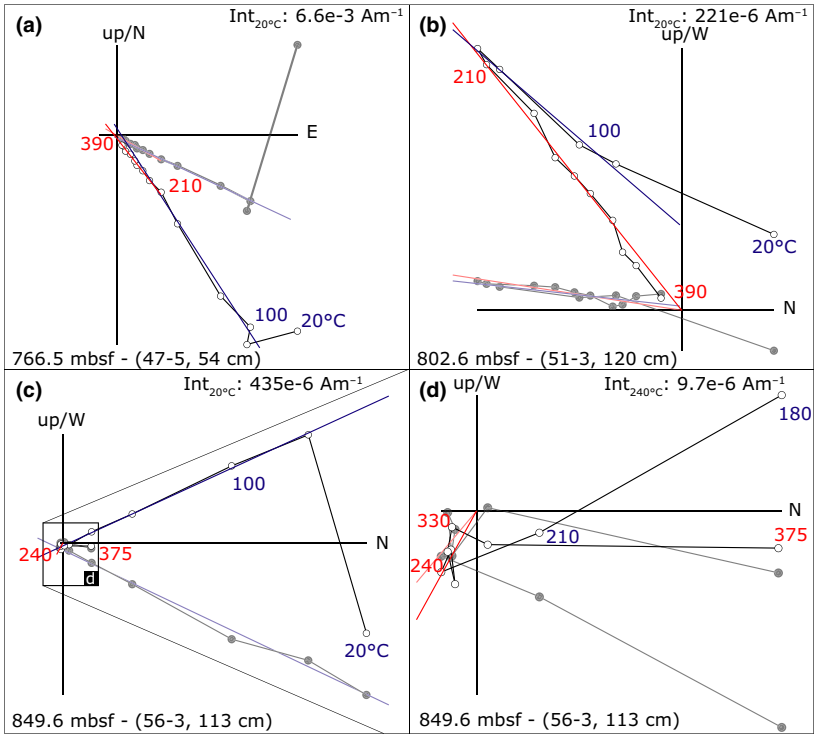

Fig. 2 (a–d) Demagnetization diagrams of representative samples. For each sample: lower left: depth in core (core-section, interval), upper right: intensity of the magnetization at the starting temperature. For each sample: in blue, the low-temperature overprint and, in red, the high-temperature primary component. All cores of DSDP leg 42B are rotary drilled; therefore, we can only use the inclination for magnetostratigraphic purposes.

age of 4.36 ± 0.19 Ma (1σ) (Fig. 3). Relevant analytical data are summarized in Table 1.

Calcareous nannofossils and diatoms

Time zonation based on microfossils is problematic in the non-marine Black Sea deposits (Percival, 1978; Ross, 1978). Among the more useful microfossil groups studied for Hole 380A are diatoms (Jousé and Mukhina, 1978; Schrader, 1978; Khursevich and Mukhina, 1995), which are very sensitive to palaeoenvironmental changes under non-marine conditions. Popescu *et al.* (2010) reported, at 840 mbsf, the occurrence of calcareous nannofossils *Triquetrorhabdulus rugosus* and *Ceratolithus acutus* and proposed an age between 5.345 and 5.279 Ma. However, this is inconsistent with the proposed age of ~6.1 Ma based on the first consistent occurrence of dinoflagellate cysts *Galeacysta etrusca* (841 mbsf) and *Caspidinium rugosum* (850 mbsf) (Grothe *et al.*, 2014). Therefore, we resampled the interval 840–856 mbsf for nannofossil assemblage analysis. Our results indicate the entire interval is barren of in situ nannofossils, lacking any taxon ascribable to the Pliocene. The supposed presence of the rare biostratigraphic markers *T. rugosus* and *C. acutus*, as previously reported (Popescu *et al.*, 2010), should be associated with other taxa constituting the common component of a typical lower Pliocene nannofossil assemblage. This is not the case in the sample at 840 mbsf, in which only rare long-range taxa and reworked forms (e.g. *Cyclicargolithus abisectus*, *Cyclicargolithus* spp.) are found. Therefore, we correlate the 840–850 mbsf interval using the tie point provided by the dinoflagellate cyst correlation of Grothe *et al.* (2014).

Messinian events in the Black Sea

Our $^{40}Ar/^{39}Ar$-dated ash layer of 4.36 ± 0.19 Ma at 706.8 mbsf constrains the age of the top of the studied interval. The base of the polarity column is constrained at 851 mbsf by the *Caspidinium rugosum* datum of 6.12 Ma (Grothe *et al.*, 2014). Based on these tie points, the magnetostratigraphy provides a straightforward correlation, with N1, N2 and N3 corresponding to chrons C3n.2n (Nunivak), C3n.3n (Sidufjall) and C3n.4n (Thvera) respectively (Fig. 4). The long reverse interval between 780 and 845 mbsf correlates to chron C3r.

The interpretation of a consistent lithological succession in the studied interval does not necessarily contradict the seismic interpretation of a large mass transport complex in this part of the core (Tari *et al.*, 2015). The seismic expression allows for the possibility of very large blocks moving short distances as consolidated blocks within the flow. In addition, blocks exceeding 150 m in height are known from similar deposits around the world (Bull *et al.*, 2009). Lithologically, this part of the core also appears to be internally consistent with, throughout the studied interval, nicely laminated diatomaceous marls and clays indicative of deep water, low-energy depositional environments (Shipboard Scientific Staff, 1978; Khursevich and Mukhina, 1995).

The average sedimentation rate in the upper half is ~8 cm ka^{-1}, lower than a recently modelled 20 cm ka^{-1} for a nearby site of similar age (Maynard *et al.*, 2012). Assuming continuous deposition throughout chron C3r results in a similar rate of ~8 cm ka^{-1}. Therefore, we use this constant sedimentation rate throughout chron C3r to convert the previously published proxy records to the new time frame (Table 2, Fig. 5). This allows us to tentatively link changes in the deep Black Sea to events on the Black Sea coast of Russia (Krijgsman *et al.*, 2010; Rostovtseva and Rybkina, 2014) and to the Mediterranean MSC (Roveri *et al.*, 2014). A temperature index given by the ratio between thermophilous elements and steppe elements is used to investigate continental climatic change (Traverse, 1978; Popescu *et al.*, 2010). Halophyte pollen abundance represents the proximity of the coastline

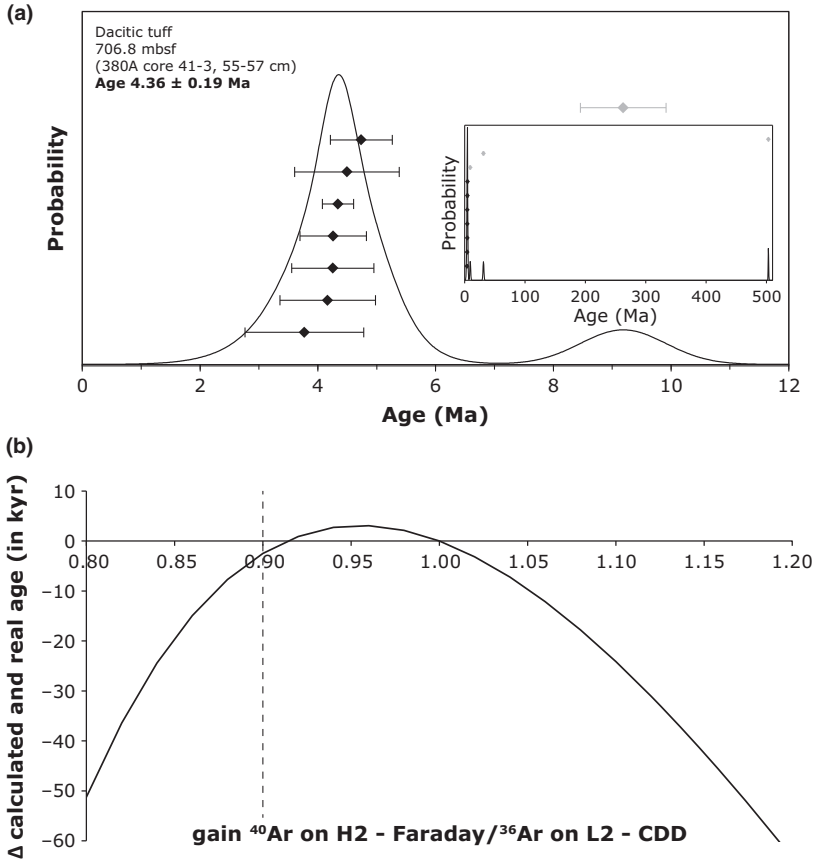

Fig. 3 (a) Individual analyses with 1 sigma error. Probability distribution is plotted on top. Weighted mean age of 7 overlapping analyses is 4.36 ± 0.19 Ma. Inset: Three out of 10 analyses are identified as outliers potentially caused by contamination with detrital material. (b) Modelled impact of the combined gain/mass discrimination correction. The five argon isotopes are measured simultaneously with ^{40}Ar on the H2-Faraday position with a 10^{12} resistor amplifier, ^{39}Ar on the H1-CDD, ^{38}Ar on the AX-CDD, ^{37}Ar on the L1-CDD and ^{36}Ar on the L2-CDD. Gain calibration for the CDDs was done by peak jumping a CO_2 reference beam (mass 43.989829) on all detectors. Background CO_2 is present in the mass spectrometer and is measured in dynamic mode, yielding an intensity of ~2–4 fA of CO_2. The CO_2 signal was too low for the Faraday detector to determine a reliable gain correction factor; therefore, we applied a combined gain/mass discrimination correction for the H2 detector by running air pipettes and simultaneous collection of ^{40}Ar on the H2 Faraday and ^{36}Ar on the L2 CDD. The correction factor H2/L2 that was derived was applied as a mass discrimination correction and therefore also influenced the other argon isotopes. We did not correct for this, but made an estimation of this correction on the final ages. Our H2/L2 gain is ~0.9 ($[CO_2]_{H2}/[CO_2]_{L2} = 0.896 \pm 0.11$), implying that our age estimate of 4.36 Ma is around 3 ka (0.07%) too young, which falls within error uncertainty and does not significantly influence the $^{40}Ar/^{39}Ar$ age.

and therefore serves as a proxy for relative sea-level (Popescu, 2006). In addition to palynological records, we use the original counts of diatom species and calculated surface-water salinity published as part of the post-cruise studies by Schrader (1978). Together, these records allow us to subdivide the Messinian deposits of DSDP Leg 42B into 4 intervals.

Interval A: Pre-evaporitic Messinian

Interval A corresponds to the pre-evaporitic Messinian and the lowermost Pontian between 6.1 Ma and ~6.0 Ma. Recovery in this part of the core is poor, but the top of this interval is located around 840 mbsf. Lithologically, this interval is predominantly composed of diatomaceous shales (Shipboard Scientific Staff, 1978). Surface salinity and sea-level are high, and temperature increases gradually, reaching a maximum prior to the onset of the MSC. The marine influx and high salinity (25–30‰) are recognized in several fossil groups and can be correlated to the so-called 'Transitional Strata' on the basin margin (Radionova and Golovina, 2011a,b). The high salinity indicates a two-way connection between the Mediterranean and the Black Sea.

Interval B: MSC Stage 1 (Primary Lower Gypsum (PLG))

A distinct change occurs at the onset of the MSC. Lithology changes, and upwards the succession is characterized by alternations of diatomaceous marls and lacustrine chalks. Palaeoenvironmental conditions change to lower surface-water salinity (0.5–5‰ or 5–18‰); increasing amounts of halophyte pollen indicate a more proximal position of the coastline (Fig. 5). During interval B, which correlates in time to stage 1 of the MSC (5.97–5.6 Ma), the palaeoenvironmental conditions remain relatively stable. Temperature in interval B is stable at a lower value than prior to the MSC, and glacial peaks TG20 and TG22 do not show up in the record as changes in the continental climate.

Interval B correlates to the Pontian highstand at the Taman Peninsula in Russia (Krijgsman *et al.*, 2010; Chang *et al.*, 2014). The presence of marine alkenones in these Pontian sediments argues for highstand conditions and two-way connectivity with the Mediterranean (Vasiliev *et al.*, 2013). In addition, around 5.8 Ma, there is a switch towards heavy δD values (Vasiliev *et al.*, 2013), which indicates a change towards a negative hydrological budget in the Black Sea or increased inflow of heavy Mediterranean waters. The lowering of salinity in interval B may have occurred under continued two-way connectivity to the Mediterranean Sea as a result of stratified water conditions in the Mediterranean during the PLG. This could have prevented the inflow of more saline water and lowered the salinity of the Black Sea.

Table 1 $^{40}Ar/^{39}Ar$ data of the total fusion experiments. Relative abundances are corrected for gain, blanks, mass discrimination and decay. Gain correction factors are based on $[CO_2]_{H1}/[CO_2]_{L2}$, $[CO_2]_{AX}/[CO_2]_{L2}$ and $[CO_2]_{L1}/[CO_2]_{L2}$ and are respectively 0.9780 ± 0.0043, 1.0006 ± 0.0040 and 1.0152 ± 0.0038 (n = 675) in all cases. $[^{40}Ar]_{H2}/[^{40}Ar]_{L2}$ is 312.04 ± 0.27 (n = 27/30), leading to a combined gain/mass discrimination correction factor of 0.98091 ± 0.00031. Fish Canyon tuff sanidine (FCs) is used as a known standard at an age of 28.201 Ma (Kuiper *et al.*, 2008). Decay constants are taken from Min *et al.* (2000), and the atmospheric air value is from Lee *et al.* (2006). The J-value is 0.0044487 ± 0.0000125 and the neutron interference corrections are $(^{39}Ar/^{37}Ar)_{Ca}$ = 0.000733 ± 0.000035, $(^{36}Ar/^{37}Ar)_{Ca}$ = 0.000265 ± 0.000008 and $(^{40}Ar/^{39}Ar)_{K}$ = 0.001340 ± 0.000787.

Lab-ID	Age ± 1σ (Ma)	$^{40}Ar^*$ (%)	$^{40}Ar^*/^{39}Ar_K$ ± 1σ	^{36}Ar ± 1σ (fA)	^{37}Ar ± 1σ (fA)	^{38}Ar ± 1σ (fA)	^{39}Ar ± 1σ (fA)	^{40}Ar ± 1σ (fA)
VU98-C48_87	3.77 ± 1.01	67.81	0.47335 ± 0.12452	0.0068 ± 0.0006	0.83 ± 14.14	0.1252 ± 0.0058	9.0887 ± 0.0097	6.2856 ± 0.0305
VU98-C48_101	4.17 ± 0.81	74.32	0.52311 ± 0.10041	0.0068 ± 0.0007	0.72 ± 14.21	0.1472 ± 0.0059	11.3970 ± 0.0113	7.9470 ± 0.0425
VU98-C48_94	4.25 ± 0.70	75.43	0.53389 ± 0.08633	0.0081 ± 0.0011	1.78 ± 14.18	0.1827 ± 0.0059	13.7497 ± 0.0116	9.6424 ± 0.1793
VU98-C48_99	4.26 ± 0.57	67.58	0.53394 ± 0.06998	0.0141 ± 0.0007	0.92 ± 14.19	0.2178 ± 0.0059	16.5512 ± 0.0121	12.9764 ± 0.1887
VU98-C48_103	4.34 ± 0.27	74.81	0.54492 ± 0.03286	0.0213 ± 0.0006	3.03 ± 14.22	0.4513 ± 0.0060	34.75966 ± 0.0219	25.0935 ± 0.0408
VU98-C48_97	4.50 ± 0.89	74.16	0.56370 ± 0.10988	0.0069 ± 0.0007	1.08 ± 14.19	0.1378 ± 0.0059	10.51908 ± 0.0099	7.9288 ± 0.1883
VU98-C48_95	4.74 ± 0.53	77.65	0.59405 ± 0.06504	0.0105 ± 0.0011	1.93 ± 14.18	0.2435 ± 0.0060	18.1897 ± 0.0161	13.7992 ± 0.1797
VU98-C48_102	9.19 ± 0.73	72.44	1.14622 ± 0.09009	0.0183 ± 0.0006	−0.05 ± 14.21	0.1690 ± 0.0059	12.6688 ± 0.0116	20.0044 ± 0.0384
VU98-C48_98	31.05 ± 0.76	96.63	3.89598 ± 0.09508	0.0054 ± 0.0006	0.34 ± 14.19	0.1570 ± 0.0059	12.1357 ± 0.0121	48.8629 ± 0.1901
VU98-C48_93	503.17 ± 0.40	99.64	72.06401 ± 0.06659	0.0239 ± 0.0012	1.53 ± 14.17	0.3648 ± 0.0060	27.7567 ± 0.0156	2007.2248 ± 0.4572

The observations in interval B indicate that the Black Sea most likely had a positive hydrological budget during this time interval.

Interval C: Stages 2 (MSC acme) and 3.1 (Upper Evaporites)

The acme of the MSC is represented sharply in the sea-level curve of DSDP Hole 380/380A, where halophytes show a rapid increase at around 5.6 Ma (800 mbsf). This sea-level drop is likely related to glacial stages TG14 and TG12. The record shows an increasingly more proximal position of the coastline, but as it is not an absolute sea-level indicator, we refrain from interpreting these data in terms of (dis)connection between the Mediterranean and (the water budget of) the Black Sea. The temperature record does not show a change in continental climate related to glacial peaks TG14 and TG12.

Diatom diversity is minimal in this interval, indicating stressed environments (Schrader, 1978). Surface salinity does not change and stays fresh. A short peak in salinity and sea-level divides the lowstand into two parts. Higher resolution studies are necessary across this interval, but this change may coincide with the transgression in the Dacian basin at the base of the Bosphorian stage at ~5.5 Ma (Stoica *et al.*, 2013). After this peak, a floral change occurs in the diatom record, indicating a change to higher trophic levels under fresh-water salinities (Schrader, 1978).

The sea-level drop in Hole 380/380A at 5.6 Ma coincides with the sea-level drop at the onset of the Kimmerian stage at the Taman Peninsula (Krijgsman *et al.*, 2010). Interestingly, sea-level in our record stays low until 5.4 Ma (792 mbsf), rather than coming back up after the two glacial peaks. A similar trend is observed in the northern and western basins in the Mediterranean, where continental clastics are found between stages 2 and 3.2 (Lago Mare) (Roveri *et al.*, 2014).

Interval D: Stage 3.2 (Lago Mare) and Pliocene

Sea-level stays low until ~5.4 Ma (790 mbsf), after which it rises to a

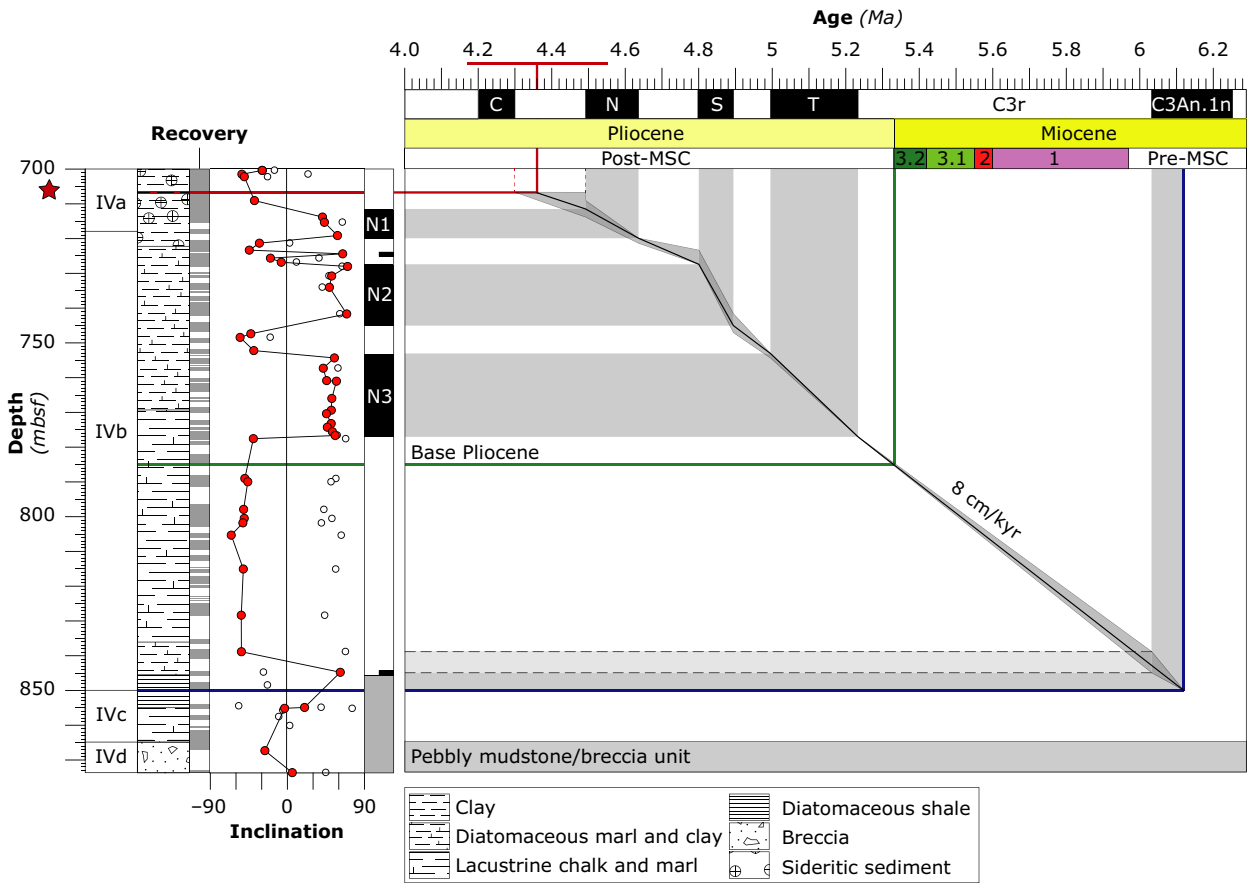

Fig. 4 Age–depth plot for the studied interval of DSDP Hole 380A, with recovered core (core breaks) in grey (white). Inclination record: closed circles: thermally demagnetized directions in the temperature range 200–400 °C used for the determination of polarity. Open circles: low-temperature (80–210 °C) overprint direction; in the interval 780–840 mbsf this consistently records an antipodal direction to the high-temperature component. These directions do not represent the original direction stored in the sediment, but rather a later, secondary remagnetization. Red star and correlation line represent level and age of the volcanic ash layer. Blue line represents *Caspidinium rugosum* dinoflaggelate cyst datum (Grothe *et al.*, 2014); dashed grey lines around 845 mbsf represent the highest normal and lowest reversed samples in the interval 840–845 mbsf.

Table 2 Age–depth tie points for the interval 700–865 mbsf used to convert the proxy records from the depth domain to the time domain. Between tie points, the sedimentation rate is assumed to be constant.

Depth (mbsf)	Age (Ma)	Type
706	4.36 ± 0.19	$^{40}Ar/^{39}Ar$
711.5	4.49	Magnetic reversal
720	4.63	Magnetic reversal
727.5	4.80	Magnetic reversal
745	4.9	Magnetic reversal
753	5	Magnetic reversal
778	5.24	Magnetic reversal
842 ± 3	6.03	Magnetic reversal
851.5	6.12	Biostratigraphic

similar level to interval B and thereafter remains stable into the Pliocene. The Mio-Pliocene boundary (5.33 Ma) should be located at around 785 mbsf (Fig. 4), but no major change is observed. Diatom diversity is low until 5.2 Ma, after which a diverse, endemic fresh-water fauna develops (Khursevich and Mukhina, 1995).

The spread of Paratethyan species across the Mediterranean during the Lago Mare at 5.4 Ma occurs roughly synchronously throughout the basin and is thought to be related to a more positive water budget in the Paratethys (Gliozzi *et al.*, 2007). At the same time, our record shows an increase in sea-level in the Black Sea.

Conclusion

We present constraints on the coevolution of the Mediterranean and Black Sea during the MSC from a basinal location in the Black Sea (DSDP Site 380/380A). Across the

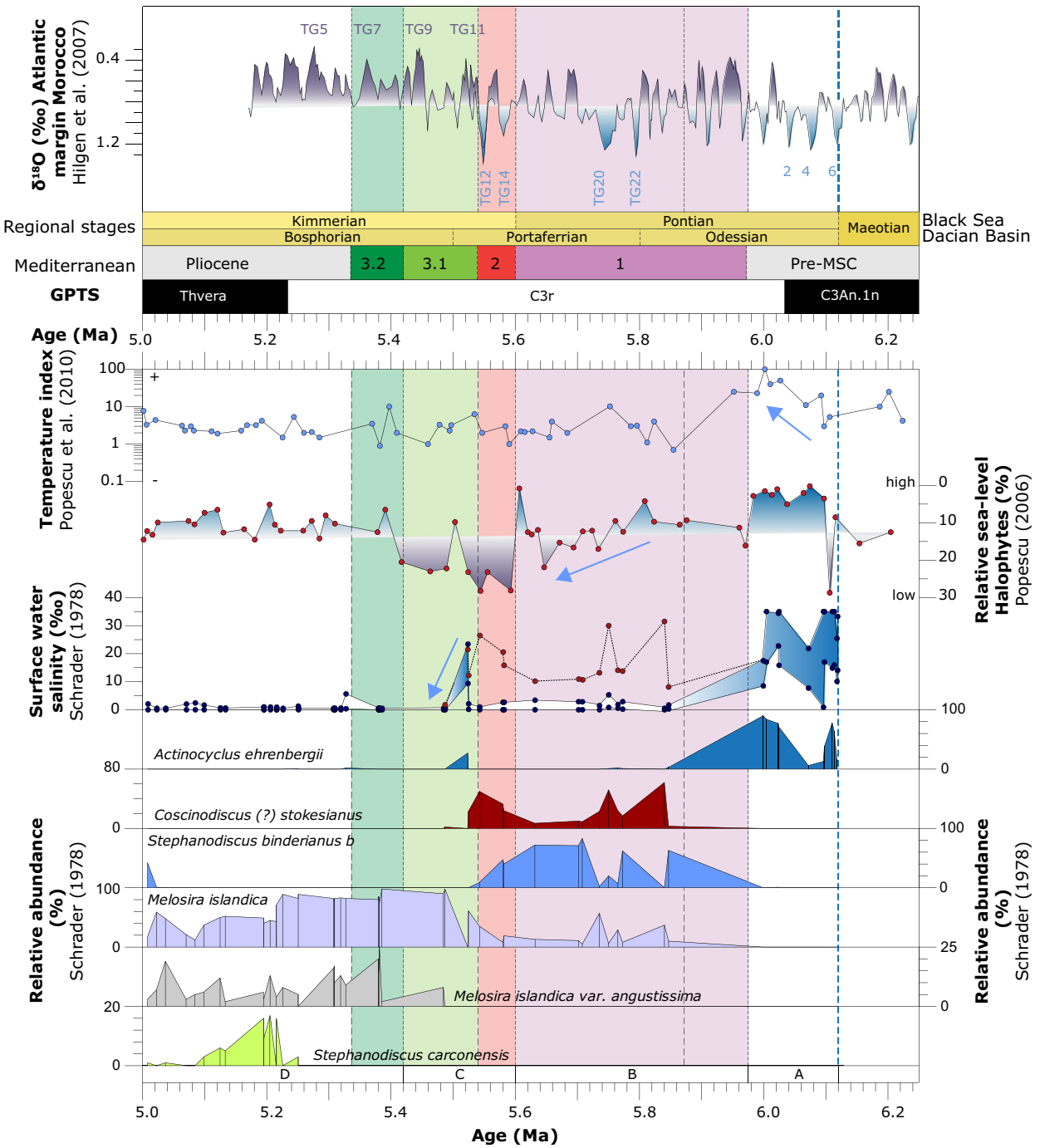

Fig. 5 Top to bottom: $\delta^{18}O$ record of the Atlantic margin of Morocco (Hilgen *et al.*, 2007) with major (inter)glacial stages indicated; Paratethyan regional stages (Krijgsman *et al.*, 2010); MSC stages (Roveri *et al.*, 2014); geomagnetic polarity and age (Hilgen *et al.*, 2012). DSDP 380A records: temperature index (Popescu *et al.*, 2010); halophyte sea-level record (Popescu, 2006); surface-water salinity (Schrader, 1978). The salinity tolerance of the diatom species was originally calculated using the highest and lowest known salinity tolerances (in blue). We give an additional upper salinity estimate (in red) based on recalculating salinity with a more marine estimate of 17 p.p.m. for *Coscinodiscus (?) stokesianus*, as proposed by Schrader (1978). Major diatom species relative abundances (in percentages, note different scales) after Schrader (1978).

MSC, the Black Sea changes from a connected marine basin to a disconnected lake. During most of the MSC, the Black Sea had a positive hydrological budget, supplying low-salinity water to the Mediterranean. Between 5.6 and 5.4 Ma, sea-level fell, but the data do not conclusively show whether this was a drop to the palaeo-Bosporus sill, or below. Sea-level rose at around 5.4 Ma in the Black Sea, coinciding

with the introduction of a diverse Paratethyan fauna throughout the Mediterranean Sea. No observable change occurs in our basinal Black Sea record across the Mio-Pliocene boundary. Getting absolute constraints on sea-level, preferably from an additional site, will be important in unravelling the detail of Mediterranean-Paratethys connectivity.

Acknowledgements

The staff members at the IODP Bremen Core Repository are thanked for their help during sampling. Roel van Elsas is acknowledged for his support during mineral separation. Research was financially supported by the Netherlands Research Center for Integrated Solid Earth Sciences (ISES) and the Netherlands Organization for Scientific Research (NWO). Two anonymous reviewers are thanked for their insightful comments, which helped to improve the manuscript.

References

Bull, S., Cartwright, J. and Huuse, M., 2009. A review of kinematic indicators from mass-transport complexes using 3D seismic data. *Mar. Pet. Geol.*, **26**, 1132–1151.

Cagatay, M.N., Görür, N., Flecker, R., Sakinc, M., Tünoglu, C., Ellam, R., Krijgsman, W., Vincent, S.J. and Dikbas, A., 2006. Paratethyan-Mediterranean connectivity in the Sea of Marmara region (NW Turkey) during the Messinian. *Sed. Geol.*, **188–189**, 171–187.

Chang, L., Vasiliev, I., Van Baak, C.G.C., Krijgsman, W., Dekkers, M.J., Roberts, A.P., Fitz Gerald, J.D., Van Hoesel, A. and Winklhofer, M., 2014. Identification and environmental interpretation of diagenetic and biogenic greigite in sediments: a lesson from the Messinian Black Sea. *Geochem. Geophys. Geosyst.*, **15**, 3612–3627.

Giovanoli, F., 1979. *Die Remanente Magnetisierung von Seesedimenten: mitteilungen aus dem Geologischen Institut der Eidg*. Technischen Hochschule und der Universitaet Zuerich, Neue Folge Nr. 230, Geologischen Institut, ETH Zurich, Zurich.

Gliozzi, E., Ceci, M.E., Grossi, F. and Ligios, S., 2007. Paratethyan Ostracod immigrants in Italy during the Late Miocene. *Geobios*, **40**, 325–337.

Grothe, A., Sangiorgi, F., Mulders, Y.R., Vasiliev, I., Reichart, G.-J., Brinkhuis, H., Stoica, M. and Krijgsman, W., 2014. Black Sea desiccation during the Messinian Salinity Crisis: fact or fiction? *Geology*, **42**, 563–566.

Hilgen, F.J., Kuiper, K.F., Krijgsman, W., Snel, E. and Van der Laan, E., 2007. Astronomical tuning as the basis for high resolution chronostratigraphy: the intricate history of the Messinian Salinity Crisis. *Stratigraphy*, **4**, 231–238.

Hilgen, F.J., Lourens, L.J. and Van Dam, J.A., 2012. The Neogene Period. In: *The Geological Time Scale 2012* (F.M. Gradstein, J.G. Ogg, M.D. Schmitz and G.M. Ogg, eds), pp. 947–1002. Elsevier BV, Amsterdam.

Hsü, K.J. and Giovanoli, F., 1979. Messinian event in the Black Sea. *Palaeogeogr. Palaeoclimatol. Palaeoecol.*, **29**, 75–93.

Jousé, A.P. and Mukhina, V. V., 1978. 42. Diatom units and the paleogeography of the Black Sea in the Late Cenozoic (DSDP, Leg 42B). In: *Initial Reports of the Deep Sea Drilling Project*, Vol. 42, Part 2 (D.A. Ross and Y.P. Neprochnov, eds), pp. 903–950. U.S. Government Printing Office, Washington.

Khursevich, G.L. and Mukhina, V. V, 1995. The evolution of diatoms of the Black Sea (on the Deep Sea Drilling Project) (in Russian). *Modern and Fossil Microplankton Oceans*, 108–114.

Krijgsman, W., Stoica, M., Vasiliev, I. and Popov, V.V., 2010. Rise and fall of the Paratethys Sea during the Messinian Salinity Crisis. *Earth Planet. Sci. Lett.*, **290**, 183–191.

Kuiper, K.F., Deino, A., Hilgen, F.J., Krijgsman, W., Renne, P.R. and Wijbrans, J.R., 2008. Synchronizing rock clocks of Earth history. *Science*, **320**, 500–504.

Lee, J.-Y., Marti, K., Severinghaus, J.P., Kawamura, K., Yoo, H.-S., Lee, J.B. and Kim, J.S., 2006. A redetermination of the isotopic abundances of atmospheric Ar. *Geochim. Cosmochim. Acta*, **70**, 4507–4512.

Maynard, J.R., Ardic, C. and McAllister, N., 2012. Source to sink assessment of Oligocene to Pleistocene sediment supply in the Black Sea. *GCSSEPM Conf. Houston Trans.*, **32**, 664–700.

Min, K., Mundil, R., Renne, P.R. and Ludwig, K.R., 2000. A test for systematic errors in 40Ar/39Ar geochronology through comparison with U/Pb analysis of a 1.1-Ga rhyolite. *Geochim. Cosmochim. Acta*, **64**, 73–98.

Nevesskaya, L.A., Goncharova, I.A., Ilyina, L.B., Paramonova, N.P. and Khondkarian, S.O., 2003. The Neogene stratigraphic scale of the Eastern Paratethys. *Stratigr. Geol. Correl.*, **11**, 105–127.

Percival, S.F., 1978. 39. Indiginous and reworked coccoliths from the Black Sea. In: *Initial Reports of the Deep Sea Drilling Project*, Vol. 42, Part 2. (D.A. Ross and Y.P. Neprochnov, eds), pp. 773–781. U.S. Government Printing Office, Washington.

Popescu, S.-M., 2006. Late Miocene and early Pliocene environments in the southwestern Black Sea region from high-resolution palynology of DSDP Site 380A (Leg 42B). *Palaeogeogr. Palaeoclimatol. Palaeoecol.*, **238**, 64–77.

Popescu, S.-M., Biltekin, D., Winter, H., Suc, J.-P., Melinte-Dobrinescu, M.C., Klotz, S., Rabineau, M., Combourieu-Nebout, N., Clauzon, G. and Deaconu, F., 2010. Pliocene and Lower Pleistocene vegetation and climate change at the European scale: long pollen records and climatostratigraphy. *Quatern. Int.*, **219**, 152–167.

Popov, S.V., Shcherba, I.G., Ilyina, L.B., Nevesskaya, L.A., Paramonova, N.P., Khondkarian, S.O. and Magyar, I., 2006. Late Miocene to Pliocene palaeogeography of the Paratethys and its relation to the Mediterranean. *Palaeogeogr. Palaeoclimatol. Palaeoecol.*, **238**, 91–106.

Radionova, E.P. and Golovina, L.A., 2011a. Upper Maeotian—Lower Pontian "Transitional Strata" in the Taman Peninsula: stratigraphic position and paleogeographic interpretation. *Geol. Carpath.*, **62**, 77–90.

Radionova, E.P. and Golovina, L.A., 2011b. Presumably Messinian deposits in the Black Sea (Sites 380A, 381 DSDP and Zheleznyi Rog section of Taman Peninsula). In: *Climate Changes, Bio-Events and Geochronology in the Atlantic and Mediterranean over the Last 23 Myr: Joint Regional Committee on Mediterranean Neogene Stratigraphy (RCMNS)-Regional Committee on Atlantic Neogene Stratigraphy (RCANS) Interim Colloquim, Sal.* p. 201.

Radionova, E.P., Golovina, L. A., Filippova, N.Y., Trubikhin, V.M., Popov, S. V., Goncharova, I. A., Vernigorova, Y. V. and Pinchuk, T.N., 2012. Middle-Upper Miocene stratigraphy of the Taman Peninsula, Eastern Paratethys. *Cent. European J. Geosci.*, **4**, 188–204.

Roberts, A. P., Chang, L., Rowan, C.J, Horng, C. -S. and Florindo, F., (2011). Magnetic properties of sedimentary greigite (Fe3S4): An update. *Rev. Geophys.*, **49**, RG1002, doi: 10.1029/2010RG000336.

Ross, D.A., 1978. 2. Black Sea stratigraphy. In: *Initial Reports of the Deep Sea Drilling Project*, Vol. 42, Part 2. (D.A. Ross and Y.P. Neprochnov,

eds), pp. 17–26. U.S. Government Printing Office, Washington.
Rostovtseva, Y. V. and Rybkina, A. I., 2014. Cyclostratigraphy of Pontian deposits of the Eastern Paratethys (Zheleznyi Rog section, Taman Region). *Mosc. Univ. Geol. Bull.*, **69**, 236–241.
Roveri, M., Flecker, R., Krijgsman, W., Lofi, J., Lugli, S., Manzi, V., Sierro, F.J., Bertini, A., Camerlenghi, A., De Lange, G., Govers, R., Hilgen, F.J., Hübscher, C., Meijer, P.T. and Stoica, M., 2014. The Messinian Salinity Crisis: past and future of a great challenge for marine sciences. *Mar. Geol.*, **352**, 25–58. doi:10.1016/j.margeo.2014.02.002
Schrader, H.-J., 1978. 41. Quaternary through Neogene history of the Black Sea, deduced from the paleoecology of diatoms, silicoflagellates, ebridians, and chrysomonads. In: *Initial Reports of the Deep Sea Drilling Project*, Vol. 42, Part 2. (D.A. Ross and Y.P. Neprochnov, eds), pp. 789–901. U.S. Government Printing Office, Washington.
Shipboard Scientific Staff, 1978. 4. Site 380. In: *Initial Reports of the Deep Sea Drilling Project*, Vol. 42, Part 2. (D.A. Ross and Y.P. Neprochnov, eds), pp. 119–291. U.S. Government Printing Office, Washington.
Stoica, M., Lazar, I., Krijgsman, W., Vasiliev, I., Jipa, D.C. and Floroiu, A., 2013. Palaeoenvironmental evolution of the East Carpathian foredeep during the late Miocene - early Pliocene (Dacian Basin; Romania). *Global Planet. Change*, **103**, 135–148.
Tari, G., Fallah, M., Kosi, W., Floodpage, J., Baur, J., Bati, Z. and Sipahioğlu, N.Ö., 2015. Is the impact of the Messinian Salinity Crisis in the Black Sea comparable to that of the Mediterranean? *Mar. Pet. Geol.*, 1–14. doi:10.1016/j.marpetgeo.2015.03.021 (in press)
Traverse, A., 1978. 44. Palynological analysis of DSDP Leg 42B (1975) cores from the Black Sea. In: *Initial Reports of the Deep Sea Drilling Project*, Vol. 42, Part 2. (D.A. Ross and Y.P. Neprochnov, eds), pp. 993–1015. U.S. Government Printing Office, Washington.
Van Baak, C.G.C., Vasiliev, I., Stoica, M., Kuiper, K.F., Forte, A.M., Aliyeva, E. and Krijgsman, W., 2013. A magnetostratigraphic time frame for Plio-Pleistocene transgressions in the South Caspian Basin, Azerbaijan. *Global Planet. Change*, **103**, 119–134.
Vasiliev, I., Krijgsman, W., Langereis, C.G., Panaiotu, C.E., Matenco, L. and Bertotti, G., 2004. Towards an astrochronological framework for the eastern Paratethys Mio-Pliocene sedimentary sequences of the Focsani basin (Romania). *Earth Planet. Sci. Lett.*, **227**, 231–247.
Vasiliev, I., Krijgsman, W., Stoica, M. and Langereis, C.G., 2005. Mio-Pliocene magnetostratigraphy in the southern Carpathian foredeep and Mediterranean-Paratethys correlations. *Terra Nova*, **17**, 376–384.
Vasiliev, I., Dekkers, M.J., Krijgsman, W., Franke, C., Langereis, C.G. and Mullender, T.A.T., 2007. Early diagenetic greigite as a recorder of the paleomagnetic signal in Miocene-Pliocene sedimentary rocks of the Carpathian foredeep (Romania). *Geophys. J. Int.*, **171**, 613–629.
Vasiliev, I., Franke, C., Meeldijk, J.D., Dekkers, M.J., Langereis, C.G. and Krijgsman, W., 2008. Putative greigite magnetofossils from the Pliocene epoch. *Nat. Geosci.*, **11**, 782–786.
Vasiliev, I., Iosifidi, A.G., Khramov, A.N., Krijgsman, W., Kuiper, K.F., Langereis, C.G., Popov, V.V., Tomsha, V.A. and Yudin, S.V., 2011. Magnetostratigraphy and radio-isotope dating of upper Miocene - lower Pliocene sedimentary successions of the Black Sea Basin (Taman Peninsula, Russia). *Palaeogeogr. Palaeoclimatol. Palaeoecol.*, **310**, 163–175.
Vasiliev, I., Reichart, G.-J. and Krijgsman, W., 2013. Impact of the Messinian Salinity Crisis on Black Sea hydrology - Insights from hydrogen isotopes analysis on biomarkers. *Earth Planet. Sci. Lett.*, **362**, 272–282.

Received 27 May 2015; revised version accepted 21 August 2015

